East European Journal of Physics. 1. 161–169 (2026)
DOI: 10.26565/2312-4334-2026-1-15 ISSN 2312-4334

INVESTIGATION OF THE ^{14}N(γ,2α)^{6}LI REACTION

Serhii Afanasiev[1], **Inna Afanasieva**[1*,2], **Kateryna Chkuaseli**[2]
[1]*National Science Center "Kharkov Institute of Physics and Technology" 1, Akademicheskaya St., 61108, Kharkiv, Ukraine*
[2]*V.N. Karazin Kharkiv National University, 4, Svoboda Sq., Kharkiv, 61022, Ukraine*
[*]*Corresponding Author e-mail: afaninna@i.ua*
Received December 5, 2025; revised February 2, 2026; accepted February 22, 2026

A digital measurement technique of points coordinates along the tracks was developed for the stereo frame photonuclear reaction data bank created in KIPT. The main procedure is the analysis of pixel intensity in the area of tracks. The ^{14}N(γ,2α)^{6}Li reaction was chosen as a test reaction for measurement. A kinematic scheme for calculating the physical parameters of the reaction was created assuming a two-particle decay mode with the formation of an intermediate excited state. Experimental data and kinematic calculation were compared. Events corresponding to the partial channel of the ^{14}N(γ,^{6}Li)^{8}Be$_0$ reaction with the subsequent two-particle decay ^{8}Be $\rightarrow$ α +α were identified and the partial cross section of this channel was measured. The energy and angular distributions of particles at each decay stage were analyzed.

Keywords: *Photonuclear reactions; Diffusion chamber; Digital measurement technique; Ground state ^{8}Be*

PACS: 25.20.-x

1. INTRODUCTION

Photoreactions on light nuclei are of particular interest to nuclear physics. They are driven by the well-known electromagnetic interaction and therefore their study provides important information about the fundamental properties of the nuclear forces. Photonuclear reactions are also important in nuclear fusion and astrophysical processes [1, 2]. It has been accepted [3, 4] that at quantum energies E_γ up to the meson threshold, nucleus absorption mainly occurs through two different reaction mechanisms: giant dipole resonance (at E_γ < 40 MeV) and quasi-deuteron photoabsorption (at E_γ > 40 MeV, where the photon wavelength is usually smaller than the nucleus size but close to the deuteron size).

The (γ,N) and (γ,NN) reactions were qualitatively explained in the framework of various modifications of these interaction mechanisms. At the same time, in various nuclear reactions, not only protons and neutrons but also other particles such as deuterons, tritons, α-particles, and other light and heavy nuclei, different in composition and properties from the initial nucleus, are observed with significant probability. This led to the development of the model of the interaction of constituent nuclear particles (nucleon associations, cluster model) [5, 6]. The use of this theory made it possible to describe such effects that could not be explained by other methods. The simple cluster model assumes that the atomic nucleus consists of two structureless fragments whose properties coincide or are close to the properties of the corresponding nuclei in the free state. The two-cluster model assumes the presence of only two separate fragments – clusters, between which all nucleons of the nucleus are redistributed. The photon does not enter into strong nuclear interactions with the target nucleus, but only electromagnetic interactions with the cluster structure, the operators of which are exactly known. Therefore, it is possible to take into account only nuclear interactions of related clusters, which greatly simplifies the consideration in comparison with the three-body problem, when it is necessary to include the nuclear interaction of the incoming particle along with intercluster forces.

The ^{14}N nucleus is of interest as an intermediate between ^{12}C and ^{16}O nuclei, which in the cluster model are considered coupled systems of 3α and 4α particles. Previously, we have studied in detail the reactions of ^{12}C(γ,3α) and ^{16}O(γ,4α) [7]. In the present work, we present information on the ^{14}N(γ,2α)^{6}Li reaction, which will provide new information on the evolution of the cluster structure, which becomes more complicated beyond α-clustering. The reaction ^{14}N(γ,2α)^{6}Li has not been studied before, but nuclear reactions with such final particles in the literature are (^{3}He + ^{11}B [8], and d + ^{12}C [9]).

2. EXPERIMENTAL TECHNIQUE

The experiment was performed using a track 4π-detector (the diffusion chamber placed in a magnetic field with a strength of 1.5 T.) [10]. The chamber was exposed to a beam of bremsstrahlung photons with a maximum energy of 150 MeV emitted from a linear electron accelerator (LUE-300). The soft component of the bremsstrahlung spectrum was removed by a beryllium filter 2.5 radiation-length units in thickness. The spectral distribution of photons was assumed to be of a Schiff form corrected for its nonuniform attenuation by the filter.

To reduce the target density, the chamber was filled with a mixture of nitrogen (15%) and helium. This experimental method makes it possible to obtain, for slow final nuclei, track lengths acceptable for measurements and sufficiently high

Cite as: S. Afanasiev, I. Afanasieva, K. Chkuaseli, East Eur. J. Phys. 1, 161 (2026), https://doi.org/10.26565/2312-4334-2026-1-15

sharpness of their image at pressures close to atmospheric pressure (1.5 atmospheres). The target–detector combination made it possible to register the products of a low-energy reaction and analyze it practically from its threshold.

The error in measuring the particle momentum depends on its magnitude and track length, and ranges from 3 to 10%. The energy of the stopped particles was determined from the range-energy relationship. The range in the mixture was obtained taking into account the ion charge exchange with the medium, using tabulated data for several target.

2.1. Digital Measurement of Point Coordinates Along Tracks

In the experiment, during the sessions of irradiation of the camera, the working area of the camera was photographed by two 2-lens cameras. A large amount of information on multiparticle photoreactions was collected and an experimental complex with a digital data bank of stereo frames and a set of graphic programs that allow to restore events and perform physical analysis of the obtained data was created [11]. Photo frames have a structured name with the maximum necessary information about the experiment session.

In [11], a method of digital semi-automatic measurement of the coordinates of points along the track was proposed. This allowed us to compare the digital method and the method using special devices. Also, the procedure of correct obtaining of physical information by digital measurement was created.

In this work, a fully automatic method of obtaining the kinematic parameters of particles is proposed, which reduces the contribution of the meter error and significantly speeds up the image processing. For this purpose, a specialized graphical application was created using the Python programming language on the platform of the Tkinter graphics library with the use of additional modules - PIL, NumPy, SciPY, and Pandas. The PIL module allows you to access a two-dimensional array of numbers, which is a function of the image intensity distribution on the plane. The intensity range is from 0 (black) to 255 (white). The coordinate system starts in the upper left corner. The X coordinate increases from left to right, and the Y coordinate increases from top to bottom. Next, we will present algorithms for the mathematical processing of digital arrays (NumPy and SciPY) with further visualization of the results.

Fig. 1 shows two identical fragments of a photo frame with a three-beam event. The white segments emanating from the same vertex correspond to a three-beam event. It should be noted that there are significant background emissions (light objects in the frame) that can cause distortions during image analysis. They arise due to the complex gas structure of the diffusion chamber. However, such background emissions are not systematic and the total intensity along the tracks should be higher.

To implement an automatic method for obtaining kinematic parameters of reaction particles, an algorithm is proposed in which the pixel intensity is scanned along a circular trajectory of a specified radius and the average intensity value is calculated at each scanning step

$$I_\theta = (\sum_{i=1}^{n} I_i)/n, \tag{1}$$

where n is the number of pixels (length radius), θ - scaning angle, and I_i - is the intensity of the i-th pixel.

In Fig. 1 above, for a visual example, dark segments of 50 pixels in length represent the procedure of scanning in a circle. The scaning was performed along the clockwise trajectory with a step of 15 degrees. In the real study, the scanning step was 1º. For the convenience of data analysis and searching for extremes, we introduced the relative intensity $I^{extr} = I_\theta / I^{aver}$, where I^{aver} - is the average intensity of the circle.

In Fig. 2, the histogram shows the dependence of I^{extr} on the scanning angle in the range from 0 to 360 degrees. There is an irregular structure with several maxima corresponding to the deviation from the background in the scanning area. To automatically determine the position of these maxima, we used the *groupby()* function from the Pandas module, which performs grouping by one or more parameters and determines the inflection points (extremes). The positions of the calculated extremes are shown as solid points. The three maxima in the positive region correspond to the three tracks in Fig. 1, and the position of the maximum gives the value of the departure angle of the corresponding track.

Thus, knowing the top of the event, the angles of departure of the tracks, and the average intensity of the I^{aver} in the selected direction, it is possible to calculate the coordinates of points along each track. For this purpose, the procedure of sequential advancement of the scanning segment along the corresponding track was performed. The pixels in the scanning segment were checked for intensity. A sharp change in intensity compared to I^{aver} made it possible to determine the boundary of the track. If all pixels corresponded to the track, the procedure was performed to move the start of the scan to the last point of the scanning segment, and then the procedure of scanning the intensity of pixels along a circular trajectory was performed again to determine the angle of departure of the track and further advancement along the track. This sequence of actions was performed in a loop until the track boundary was determined. This algorithm allows us to take into account the curvature of the track and at each stage of moving along the track it is possible to refine the departure angle.

In Fig. 1 on the bottom image shows the result of the automatic digitization of all three event tracks. The points describe the trajectory of the tracks well. Subsequently, we performed the functions of fitting the points with a second-order linear curve and refining the coordinates of the middle of the track. After reconstructing the geometry of the event, a

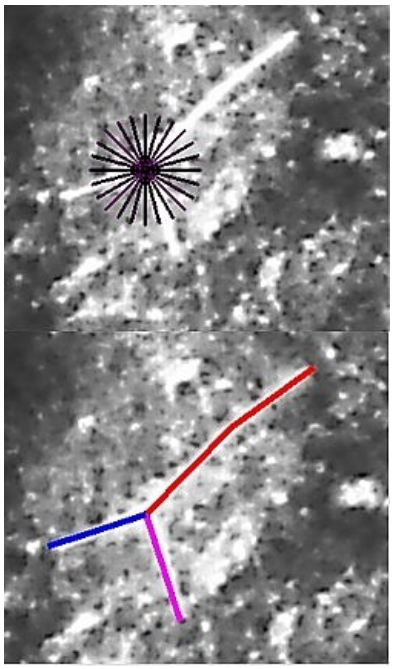

Figure 1. Digital image processing.

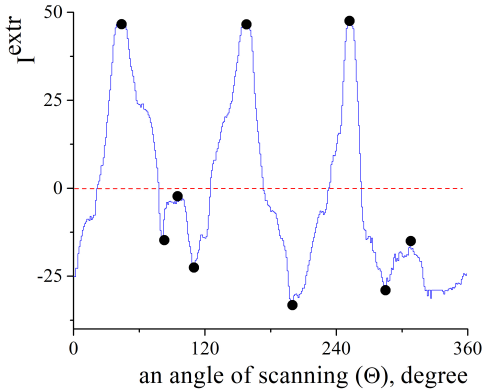

Figure 2. Dependence of pixel intensity on scanning angle.

numerical matrix of this event is created, in which for each track there are guide cosines l, m, n; the radius of curvature and track length.

2.2. $^{14}N(\gamma,2\alpha)^{6}Li$ Reaction Events

For the measurement and processing of the $^{14}N(\gamma,2\alpha)^{6}Li$ reaction, we selected 3-ray stars close to compatibility, two of whose rays belong to two-charged particles and one to a three-charged particle. The ionization density, its change along the track at a known momentum, makes it possible to determine the charge of the particle. This identification was performed visually at the stage of selecting events for measurements. The particle tracks usually ended in the working area of the chamber, so the experimental data of their energy losses (the range-energy relationship) were used to determine the kinetic energy of the particles [12].

The methodology for selecting events is traditional for this method of experiment and has been previously described [13, 14].

Events corresponding to the $^{14}N(\gamma,2\alpha)^{6}Li$ reaction were selected after measurements based on the momentum balance. Boundary conditions were imposed on the quantities $\sum P_x^i$, $\sum P_y^i$, and $\sum P_z^i$, where $P^i_{x(y,z)}$ - are the components of the three-dimensional momentum of the i-th final particle. The projection of the imbalance onto the OX axis, along which the γ-quanta is directed, is equal to the sum of the projections of the momentum onto this axis minus the energy

of the γ-quanta, which was defined as the sum of the kinetic energies of the final particles and the reaction threshold. A clearly pronounced peak in the distributions for $\sum P_{x(y,z)}$ in region 0 corresponds to the events of the examined reaction. The laws of conservation of energy and momentum make it possible to refine the measurement results of one of the tracks, usually the worst measured one. The measurement error of the momentum of charged particles depends on its size and track length and ranges from 3 to 10%.

3. DATA PROCESSING

For the $^{14}N(\gamma,2\alpha)^{6}Li$ reaction events, the excitation energy of a pair of particles was determined as

$$E_x(\alpha\alpha) = M^{eff} - (2m_\alpha) \tag{2}$$

where M^{eff} is effective mass equal to the total energy of a pair of α-particles in their resting state, and m_α is the mass of the α-particle.

In Fig. 3, the histogram shows the distribution of $E_x(\alpha\alpha)$ with a step of 0.25 MeV. The distribution has a structure: a narrow near-threshold maximum and a concentration of events in the region of 3 MeV. The area of the first maximum is 15% of the total area. There are three particles in the final state of the reaction, so three combinations of particle-pair systems are possible. This means that the structure observed in Fig. 3, is formed either by the decay of the intermediate excited state of the ^{8}Be nucleus or is simulated by one of the background pairs during the decay of the intermediate excited state of the ^{10}B nucleus.

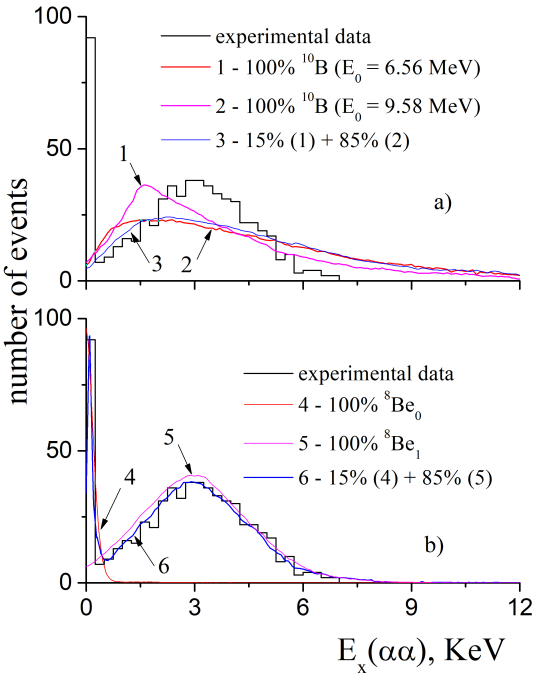

Figure 3. Distribution of events by excitation energy of 2α-particles. The curves are explained in the text

3.1. Kinematic Calculation

Experimental studies of nuclear reactions on light nuclei are usually accompanied by a mathematical model of the process under study [15-16].

To analyze the experimental data and compare it with the kinematic calculation, a graphical application in the Python programming language was created for this work. The matplotlib library is used for data visualization.

The kinematic model of the $^{14}N(\gamma,2\alpha)^{6}Li$ reaction was developed under the assumption of two-particle decay with the formation of an intermediate excited state. In the system of the center of mass (s.c.m.) of a two-particle reaction, the kinematics is determined by the fact that, regardless of the specific type of interaction, the reaction products scatter at an angle of 180° and have equal modulus momentum, and their energies in the same system depend only on the masses of the particles and the total energy of the system.

For the reaction of $^{14}N(\gamma,2\alpha)^{6}Li$, decay through two channels is possible:

$\gamma + {}^{14}N \rightarrow \alpha_1 + {}^{10}B^* \rightarrow \alpha_1 + \alpha_2 + {}^6Li$ (I)

and

$\gamma + {}^{14}N \rightarrow {}^6Li + {}^8Be^* \rightarrow \alpha_1 + \alpha_2 + {}^6Li$ (II)

The mathematical calculation is based on the literature data on the parameters of the levels of ^{10}B and ^8Be nuclei [17] and the corresponding assumptions about the angular distributions in the system of the reaction center of the particle that first left the ^{14}N nucleus and the particles in the intermediate state resting state. Each decay mode is reduced to three two-particle systems:

- $(\gamma + {}^{14}N)$ – the initial,
- $(\alpha + {}^{10}B^*)$ or $({}^6Li + {}^8Be^*)$ – the intermediate,
- $({}^6Li + \alpha)$ or $(\alpha + \alpha)$ – the final.

To generate random values, a set of functions of the standard random library of the Python programming language was used. Several excited states of ^{10}B and ^8Be nuclei can contribute to the reaction. A scheme was created that allows you to select both the relative contribution for each channel (1) or (2) and the contribution of a separate level in each channel. To do this, we used the random.randint(0,100) function, which creates random, uncorrelated numbers evenly distributed in the range from 0 to 100. For the initial system, the numerical function of the distribution of the number of events on the energy of quanta $N(E_\gamma)$ was taken from a real experiment, and random values of E_γ were generated by the random.choice() function. The excitation curves $f(E_x)$ of the ^{10}B and ^8Be states of the nuclei were taken as Gaussian functions with a maximum position E_0 and half-width at half-height (σ) from a compilation of spectroscopic data [17]. Random values were generated by the function random.gauss(E_0,σ).

In the non-relativistic approximation, in the case of a two-particle channel, the law of conservation of energy is $E_\gamma = T_{P1} + T_{P2} + E_x + Q$, where T is the kinetic energy of particles P_1 and P_2 ($P_1 = \alpha_1$, $P_2 = {}^{10}B$ or $P_1 = {}^6Li$, $P_2 = {}^8Be$), E_x is the excitation energy of the intermediate particle ($E_x({}^{10}B)$ in the case of channel (I) or $E_x({}^8Be)$ for channel (II)), and Q is the energy threshold of the corresponding channel.

Using a two-particle channel and an unambiguous connection between the particles, we obtain:

$$T_{P1} = \frac{M_{P1}}{M_{P1} + M_{P2}}(E_\gamma - Q - E_x) \tag{3}$$

After the procedures for generating E_γ and E_x, T_{P1} and, accordingly, the particle momentum P_{P1} was determined.

The distributions over the polar angle θ for particle P_1 were taken in form $f(\theta)=c_1 sin^2\theta + c_2 sin^2\theta cos\theta + c_3 sin^2\theta cos^2\theta + c_4$, where c_{1-4} - are coefficients containing information about the reaction mechanism and wave functions of the nuclei. Parameters c_{1-4} were determined from the quantum values of the intermediate excited nucleus [18]. The distribution in the azimuthal angle ϕ is isotropic and was generated by multiplying the random number random.randint(0,1) by 2π.

The longitudinal and transverse projections of the particle P_1's momentum were determined, based on the generated values of the polar (θ) and azimuthal (ϕ) angles. The values of the projections and the total momentum of nucleus P_2 were calculated from the two-particle process.

A similar procedure was carried out for the final system, provided that the energy of the system is the excitation energy of the particle P_2. The kinematic parameters of the particles were transferred from the s.c.m. reaction to the laboratory system. The laws of conservation of energy and momentum for the kinematic parameters of the particles were checked. An event was considered formed if it satisfied the conservation laws.

3.2. Decay Channel Identification

For example, let us compare the kinematic calculation with the experiment (Fig. 3). Using the kinematic model, we constructed several distributions of events according to $E_x(\alpha\alpha)$ under the assumption of each decay channel - (I) or (II).

In Fig. 3a, three curves are presented in the framework of decay through a channel (I): curve 1 - with 100% production of the narrow ^{10}B nucleus level (E_0 = 6.56 MeV, σ = 0.025 MeV); curve 2 - with 100% formation of the broad ^{10}B nucleus level (E_0 = 9.58 MeV, σ = 0.257 MeV); curve 3 - with 15% of the narrow ^{10}B nucleus level and 85% of the broad ^{10}B nucleus level formation. Level parameters are taken from a compilation of spectroscopic data [17]. The dependence of 15% and 85% is taken from the ratio of the areas of the maxima of the distribution of the number of events for $E_x(\alpha\alpha)$ in the experiment (Fig. 3, histogram). The calculated curves were normalized to the experimental area distribution. The curves do not fully describe the near-threshold maximum at $E_x(\alpha\alpha) < 0.25$ MeV. In addition, they give only one maximum, which has almost the same position (at ~ 1.5 MeV) with different widths. It was checked that any combinations of the relative contributions of curves 1 and 2 also do not describe the experimental distribution.

Two levels of ^8Be nucleus were chosen for a channel (II): the ground state (GS) with E_0 = 0.092 MeV, σ = 0.025 MeV, and 1^{st} excited state with E_0 = 3.04 MeV, σ = 0.75 MeV. Fig. 3b shows three curves corresponding to the following ratios: curve 4 - with 100% GS; curve 5 - with 100% of the 1^{st} level of the ^8Be nucleus; curve 6 - with 15% GS and 85% of the 1^{st} level of the ^8Be nucleus. Curves 4 and 5 are consistent with the experiment when describing the first and second maxima, respectively. And curve 6 satisfactorily describes the total experimental distribution. Thus, it can be concluded that in the $^{14}N(\gamma,2\alpha)^6Li$ reaction, decay occurs mainly through the formation of an intermediate excited ^8Be nucleus.

4. ^{8}BE GROUND STATE FORMATION CHANNEL

The maximum up to 0.25 MeV (Fig. 3) is shown in Fig. 4b as data points with a 20 keV step. The errors are statistical. A fit was performed using a Gaussian distribution (solid curve) with a peak position E_0 = 0.096 ± 0.005 MeV and full width at half maximum σ = 0.064 ± 0.01 MeV. From spectrometric measurements [17], it is known that the parameters of the ground state (GS) of the ^{8}Be nucleus: E_0 = 0.092 MeV, Γ = 5.57 eV, quantum numbers - $J^\pi = 0^+$.

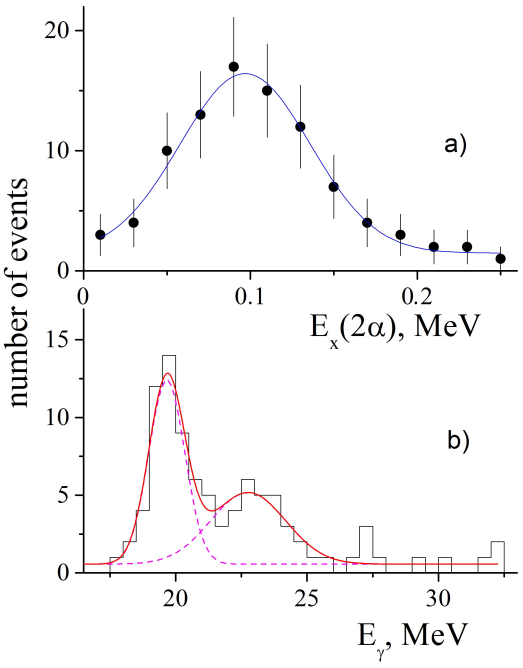

Figure 4. a) ground state ^{8}Be nucleus, b) partial cross-section of the channel for the formation of the ground state of the ^{8}Be nucleus in the ^{14}N(γ,2α)^{6}Li reaction.

The positions of the maxima (experimental and tabular) coincide within the error. Therefore, the concentration of events in the region of 0.1 MeV can be explained by the formation of the GS of the ^{8}Be nucleus. Due to insufficient energy resolution and low statistical power, the task of specifying the GS parameters was not set in this experiment. The width observed in this experiment is instrumental. Events (N^{GS}), in which a pair of α-particles corresponds to the formation of the GS of the ^{8}Be, nucleus, are reliably distinguished. The relative yield of this partial channel is – η=14.98% (η=N^{GS}/N, where N – is the total number of reaction events). The histogram in Fig. 4b presents the partial cross-section for the formation channel of the ^{8}Be nucleus GS in the ^{14}N(γ,^{6}Li)^{8}Be$_0$ reaction with a 0.5 MeV step for E_γ. A structure is observed in the distribution. The solid line shows the fit of the cross-section with a combination of two Gaussian functions (dashed lines), which resulted in the determination of the energy positions of the maxima and their widths - $E_\gamma{}^1$ = 19.66 ± 0.25 MeV, Γ^1 = 1.25 ± 0.29 MeV and $E_\gamma{}^2$ = 22.75 ± 0.42 MeV, Γ^2 = 2.79 ± 0.51 MeV.

Sequential two-particle decay allows us to determine the energy and angular distributions at each stage of decay.

In Fig. 5a, solid circles are used to exhibit the dependence of the number of events on the escape angle of the GS of ^{8}Be nucleus, θ(^{8}Be), in the center of the mass coordinate frame for the reaction in whole. After, the circles are drawn in the middle of the histogram steps, and vertical bars mark statistical errors. The figure demonstrates that the GS of ^{8}Be nucleus yield is symmetric about 90° and looks similar to $sin^2\theta cos^2\theta$. We performed the Legendre polynomial fit:

$$f(\theta) = a \cdot f_1 + b \cdot f_2 + c \cdot f_3 + d \cdot f_4 \tag{4}$$

where a, b, c, d – are coefficients containing information about the reaction mechanism and wave functions of the nuclei, and, $f_1 = sin^2\theta$, $f_2 = sin^2\theta cos\theta$, $f_3 = sin^2\theta cos^2\theta$, f_4 =1. In the figure, the solid curve represents the function f(θ) with a = 3.84 ± 0.87, b = 0.23 ± 1.98, c = 39.29 ± 4.35, d = 0.46 ± 0.55. For the parameters b and d, the values and errors of their measurements are close and their contribution to the fit is insignificant. The main contribution is given by the parameter c. The data obtained allows us to estimate the multipole amplitudes of the photoprocess in the future, since for this two-particle process we know the spin-parity of the particles - 1^+ for ^{6}Li and 0^+ for ^{8}Be.

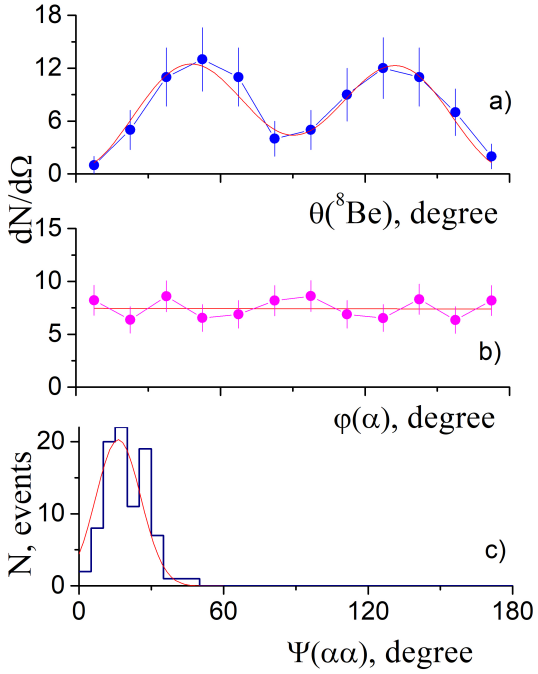

Figure 5. a) event distribution over the escape angle of the GS of the ^{8}Be nucleus, b) angular distributions of α-particles in the system of the center of mass of the ^{8}Be nucleus, c) dependence of the angle of separation of two α-particles.

In Fig. 5b, the solid circles represent the angular distributions of α-particles in the system of the center of mass of the ^{8}Be nucleus. The polar angle ($\phi(\alpha)$) is reckoned from the direction of the ^{8}Be nucleus motion. The angular distributions are isotropic (solid line in Fig. 3b is a fit with a linear function with a slope of -0.004 ± 0.012). This means that the orbital momentum l=0. It follows that the quantum numbers $J^{\pi} = 0^{+}$, is in the GS of ^{8}Be nucleus.

In Fig. 5c, the histogram shows the distribution of the number of events as a function of the angle of departure (ψ) of the α-particle pair. Fitting with the Gaussian function gave the values of the maximum and width at the half-height - $\psi_0 = 16.28^{\circ} \pm 0.71^{\circ}$ and $\Gamma(\psi) = 18.71^{\circ} \pm 1.52^{\circ}$.

The relative energies of α-particles were determined as the ratio:

$$\epsilon_i = T_i/T_0 \tag{5}$$

where i – is the particle identifier.

To test the possible mechanisms of interaction of the γ-quantum with the nucleus, the particles forming in the GS of ^{8}Be nucleus were sorted by energy for each event as $T_{\alpha}^{max} > T_{\alpha}^{min}$.

Fig. 6a demonstrates the distribution of the number of events over the relative energy ϵ for the α-particles (squares - $\epsilon(\alpha^{min})$, circles - $\epsilon(\alpha^{max})$ and asterisks - $\epsilon(^{6}\text{Li})$. The distributions were fitted with the Gaussian function and the values of the corresponding maxima were obtained: - $\epsilon(\alpha^{min}) = 0.17 \pm 0.03$, $\epsilon(\alpha^{max}) = 0.25 \pm 0.03$, $\epsilon(^{6}\text{Li}) = 0.55 \pm 0.02$. The slight deviation between α^{min} and α^{max}, taking into account the small value of the angle of separation between α-particles (Fig. 5c), explains the formation of a narrow near-threshold state (Fig. 3a).

Details of the mechanisms of the channel of formation of the GS of the ^{8}Be nucleus can be studied with the help of the symmetric Dalitz plot. This technique is particularly suitable for the geometric visualization of the decay into three particles with identical masses and makes it possible to illustrate the population of the available phase space at three-body decays. If the decay is a true direct 3-particle decay, the distribution of events in the Dalitz diagram must be uniform. However, as a rule, 3-particle decays occur via resonances, i.e., the excited particle decays into a resonance and α-particle, and then the resonance, in turn, decays into two other particles. In this case, the distribution of events in the Dalitz diagram reveals an essentially non-uniform structure, with an increased concentration of events in the region of invariant masses coinciding with the resonance masses.

The Dalitz diagram is a convenient tool for studying the dynamics of 3-particle decays. The Cartesian coordinates for plotting a Dalitz diagram can be obtained as follows [10]:

$$x = \sqrt{3}(\epsilon_j - \epsilon_k); y = 2\epsilon_i - \epsilon_j - \epsilon_k \tag{6}$$

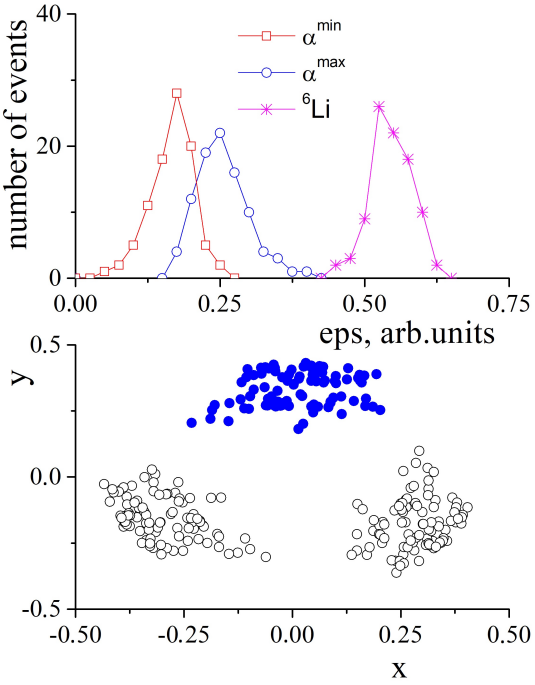

Figure 6. a) dependence of the number of events on the relative energy of particles ϵ, b) Dalitz diagram for the channel of formation of the GS of the ^{8}Be nucleus.

By definition, the sum of the relative energies of three particles equals 1. In our experiment, the contribution of each component can be evaluated from the general plot.

In Fig. 6b, the solid dots represent the dependence in the case where α-particles were used in the x coordinate, and the open dots represent combinations with ^{6}Li. The Dalitz distribution confirms the presence of an intermediate excited particle (^{8}Be) and correlates with the distribution in Fig. 6a.

5. CONCLUSIONS

A systematic study of the ^{14}N(γ,2α)^{6}Li reaction was performed. To obtain the physical parameters of the events, a graphical application was created in the Python programming language with the ability to automatically measure the coordinates of points along the tracks on digital photo frames. The main procedure is the analysis of the pixel intensity in the track area along a circular trajectory of a certain radius.

The excitation energy of the 2α-particle system was determined and a structure with two maxima was found in the distribution of the number of events by $E_x(\alpha\alpha)$. It was assumed that this structure is formed either as a result of the decay of the intermediate excited state of the ^{8}Be nucleus or is simulated by one of the background pairs during the decay of the intermediate excited state of the ^{10}B nucleus.

A kinematic scheme for calculating the physical parameters of the reaction has been created assuming a two-particle decay mode with the formation of an intermediate excited state. A comparison of experimental data and kinematic calculation has been performed and it has been determined that with high probability the decay process with the formation of an intermediate excited nucleus ^{8}Be in the ground and 1^{st} excited states occurs.

In the distribution of events by the energy of the relative motion of two a particles, a resonance was found, identified as the ground state of ^{8}Be nucleus. Events corresponding to the partial channel of the ^{14}N(γ,^{6}Li)^{8}Be$_0$ reaction with the subsequent two-particle decay ^{8}Be $\rightarrow \alpha + \alpha$ were identified and the partial cross section of this channel was measured. An analysis of the energy and angular distributions of particles at each stage of decay was performed.

ORCID

Serhii Afanasiev, https://orcid.org/0000-0003-1682-4621; **Inna Afanasieva**, https://orcid.org/0000-0002-9523-9780; **Kateryna Chkuaseli**, https://orcid.org/0009-0008-1972-9148

REFERENCES

[1] A. Coc, C. Angulo, E. Vangioni-Flam, P. Descouvemont, and A. Adahchour, Nucl. Phys. A, **752**, 522 (2005). https://doi.org/10.1016/j.nuclphysa.2005.02.057.

[2] F.-K. Thielemann, F. Brachwitz, C. Freiburghaus, *et al.*, Prog. Part. Nucl. Phys. **46**, 22 (2001). https://doi.org/10.1016/S0146-6410(01)00103-X.

[3] E.G. Fuller, Physics Reports, **127**, 185 (1985). https://doi.org/10.1016/0370-1573(85)90145-0

[4] D.J.S. Findlay, Nucl. Instr. and Meth. in Phys. Res. Section B: Beam Interactions with Materials and Atoms, **50**, 314 (1990). https://doi.org/10.1016/0168-583X(90)90374-4

[5] O.F. Nemets, V.G. Neudachin, and A.T. Rudchik, *et al.*, (Naukova Dumka, Kiyev, 1988). (in russian)

[6] M. Freer, H. Horiuchi, Y. Kanada-En'yo, *et al.*, Rev. Mod. Phys. **90**, 035004, (2018). https://doi.org/10.1103/RevModPhys.90.035004

[7] S.N. Afanasyev, Ukrainian Journal of Physics, **64**, 787 (2019). https://doi.org/10.15407/ujpe64.9.787

[8] F.C. Young, P.D. Forsyth, and J.B. Marion, Nucl. Phys. A, **91**, 209, (1967). https://doi.org/10.1016/0375-9474(67)90462-9

[9] L. Jarczyk, B. Kamys, Z. Rudy, *et al.*, Nucl. Phys. A, **459**, 52, (1986). https://doi.org/10.1016/0375-9474(86)90055-2

[10] Yu.M. Arkatov, P.I. Vatset, V.I. Voloshchuk, *et al.*, Prib. Tekh. Eksp. **3**, 205, (1969). (in russian).

[11] S.N. Afanasiev, and I.A. Afanasieva, Problems of Atomic Science and Technology, Series "Nuclear Physics Investigations", (5)(141), 87, (2022). https://doi.org/10.46813/2022-141-087

[12] O.F. Nemets, and Yu.V. Gofman, (Naukova Dumka, Kiyev, 1975). (in russian).

[13] V.V. Kirichenko, A.F. Khodyachikh, P.I. Vatset, *et al.*, Yad. Fiz. **29**, 572, (1979).

[14] S.N. Afanasyev, and A.F. Khodyachikh, Yad. Fiz. **71**, 1859, (2008). https://doi.org/10.1134/-S106377880811001X

[15] D. Dell'Aquila, I. Lombardo, and G. Verde, *et al.*, Phys. Rev. Lett. **119**, 132501, (2017). https://doi.org/10.1103/PhysRevLett.119.132501

[16] S.N. Afanasyev, in: *Proceedings of the 5rd International Conference "Computer modeling of high-technology (CMHT-2018)*, (2018), pp.37.

[17] D.R. Tilley, J.H. Kelley, J.L. Godwin, *et al.*, Nucl. Phys. A, **745**, 155, (2004). https://doi.org/10.1016/j.nuclphysa.2004.09.059

[18] A.M. Baldin, V.I. Gol'danskii, V.M. Maksimenko, and I.L. Rosenthal, *Kinematics of nuclear reactions*, (Atomizdat, Moscow, 1968). (in russian).

ДОСЛІДЖЕННЯ РЕАКЦІЇ $^{14}N(\gamma,2\alpha)^{6}Li$

Сергій Афанасьєв[1], **Інна Афанасьєва**[1,2], **Катерина Чкуаселі**[2]

[1]*Національний Науковий Центр "Харківський Фізико-Технічний Інститут", вул. Академічна, 1, 61108, Харків, Україна*

[2]*Харківський національний університет ім. В.Н. Каразіна, майдан Свободи, 4, 61022, Харків, Україна*

Для створеного в ННЦ ХФТІ банку даних стереокадрів фотоядерних реакцій розроблено методику цифрового вимірювання координат точок уздовж треків. Основною процедурою є аналіз інтенсивності пікселів в області треків. Як тестову для вимірювання обрано реакцію $^{14}N(\gamma,2\alpha)^{6}Li$. Створено кінематичну схему розрахунку фізичних параметрів реакції в припущенні двочастинкової моди розпаду з утворенням проміжного збудженого стану. Виконано порівняння експериментальних даних і кінематичного розрахунку. Виділено події, що відповідають парціальному каналу реакції $^{14}N(\gamma,^{6}Li)^{8}Be_0$ з наступним двочастинковим розпадом $^{8}Be \rightarrow \alpha + \alpha$ і виміряно парціальний перетин цього каналу. Виконано аналіз енергетичних і кутових розподілів частинок на кожному етапі розпаду.

Ключові слова: *фотоядерні реакції; дифузійна камера; цифрова техніка вимірювання; основний стан ядра* ^{8}Be